

<https://helda.helsinki.fi>

KIT pathway upregulation predicts dasatinib efficacy in acute myeloid leukemia

Malani, Disha

2020-07-17

Malani , D , Yadav , B , Kumar , A , Potdar , S , Kontro , M , Kankainen , M , Javarappa , K K , Porkka , K , Wolf , M , Aittokallio , T , Wennerberg , K , Heckman , C A , Murumägi , A & Kallioniemi , O 2020 , ' KIT pathway upregulation predicts dasatinib efficacy in acute myeloid leukemia ' , *Leukemia* , vol. 34 , no. 10 , 34 , pp. 2780 2784 . <https://>

<http://hdl.handle.net/10138/323955>

<https://doi.org/10.1038/s41375-020-0978-7>

acceptedVersion

Downloaded from Helda, University of Helsinki institutional repository.

This is an electronic reprint of the original article.

This reprint may differ from the original in pagination and typographic detail.

Please cite the original version.

1 **KIT pathway upregulation predicts dasatinib efficacy in acute myeloid leukemia**

2

3 Disha Malani¹, Bhagwan Yadav¹, Ashwini Kumar¹, Swapnil Potdar¹, Mika Kontro^{1,2,3},
4 Matti Kankainen², Komal K. Javarappa¹, Kimmo Porkka^{2,3}, Maija Wolf¹, Tero
5 Aittokallio^{1,4}, Krister Wennerberg^{1,5}, Caroline A. Heckman¹, Astrid Murumägi¹, Olli
6 Kallioniemi^{1,6}

7

8 1. Institute for Molecular Medicine Finland (FIMM), HiLIFE, University of Helsinki,
9 Helsinki, Finland

10 2. Hematology Research Unit Helsinki, University of Helsinki, Helsinki, Finland

11 3. Department of Hematology, University Hospital Comprehensive Cancer Center,
12 Helsinki, Finland

13 4. Department of Cancer Genetics, Institute for Cancer Research, Oslo University
14 Hospital, and Oslo Centre for Biostatistics and Epidemiology, University of Oslo,
15 Oslo, Norway

16 5. Biotech Research & Innovation Centre, BRIC and Novo Nordisk Foundation Center
17 for Stem Cell Biology, DanStem, University of Copenhagen, Copenhagen, Denmark

18 6. Science for Life Laboratory, Department of Oncology and Pathology, Karolinska
19 Institutet, Solna, Sweden

20

21 **Keywords:** acute myeloid leukemia, dasatinib, molecular profiling, high-throughput
22 drug testing, pathway dependency, RNA-sequencing

23 **Corresponding author:** Disha Malani

24 Institute for Molecular Medicine Finland (FIMM), University of Helsinki,

25 Address: Biomedicum 2U, Tukholmankatu 8,

26 FIN-00290 Helsinki, Finland

27 Email: disha.malani@helsinki.fi

28 Phone: +358440341101

29

30 **Text word count:** 1486/1500

31 **Figures:** 2/2

32 **References:** 15/15

33 **Supplementary Figures:** 7

34 **Supplementary Tables:** 9

35

36 **Conflicts of Interest:**

37 The authors declare no competing financial interests for this work. The senior authors
38 have received collaborative research grants for other projects as listed: OK received
39 research funding from Vinnova for collaboration between Astra-Zeneca, Takeda,
40 Pelago and Labcyte. OK is also a board member and a co-founder of Medisapiens and
41 Sartar Therapeutics and has received a royalty on patents licensed by Vysis-Abbot. KP
42 received honoraria and research funding from Bristol-Myers Squibb, Celgene, Novartis
43 and Pfizer. CH received honoraria from Celgene, Novartis and Roche and research
44 funding from Celgene, Novartis, Oncoceptides, Pfizer and the IMI2 project
45 HARMONY. KW received research funding from Novartis and Pfizer. MKo: research
46 funding from AbbVie.

Acute myeloid leukemia (AML) is an aggressive malignant disease with a poor prognosis. Although the recent approval of several new targeted drugs provides new treatment options for subsets of patients, molecular heterogeneity in AML still poses a major challenge for the patient treatment¹. Novel treatments are needed to cover the entire molecular spectrum of the disease. We and others have previously shown that functional *ex vivo* drug testing of patient-derived primary AML cells provides additional insights on the potential utility of e.g. dasatinib, venetoclax and dexamethasone for treatment of subsets of AML patients²⁻⁵. However, in most cases, the mechanism of action and the specific subgroups and biomarkers associated with the drug effects have remained unknown. Cell lines originating from different cancer types have provided valuable information about the complexity of cancer at the genomic, epigenomic, transcriptomic and drug response level⁶⁻⁹, including observations in AML^{10, 11}. However, the representability of the AML cell lines of patient AML specimens has remained unclear. Here, we aimed to i) integrate and compare pharmacological profiles between AML cell lines and patient samples to identify differential drug sensitivities; and ii) define molecular determinants and biomarkers of drug response by the integration of *in vitro*, *ex vivo* and *in vivo* patient data, focusing on KIT pathway and its inhibitors.

We compared drug response profiles between *ex vivo* AML patient samples (n=45) (Table S1) and established AML cell lines (n=28) (Table S2) using high-throughput drug sensitivity and resistance testing (DSRT) with 290 approved and investigational oncology compounds (Table S3). Drug responses were quantified as drug sensitivity score (DSS)¹². Briefly, DSS is a quantitative measurement of drug response to define drug efficacy using dose-response parameters. The differential drug sensitivity score

(dDSS) for each sample was based on comparing the DSS for that sample with the mean over all patient samples (Table S4) or mean over all cell lines (Table S5). The mutation spectrum of the AML cell lines was obtained from cancer gene panel sequencing (Table S6) while exome sequencing was applied to the patient samples and analyzed as described previously². RNA-seq data for the AML patient specimens were generated and analyzed as described previously¹³ and for the AML cell lines obtained from a published study⁹.

We first compared drug sensitivity patterns between *ex vivo* AML patient samples and cell lines using the Wilcoxon rank-sum test to reveal differential sensitivity across all drugs (Table S7). Higher efficacy for many cytotoxic chemotherapeutic drugs in the cell lines (Fig 1a) was likely due to the higher proliferation rate during drug testing as compared to the patient cells (Fig S1a). Therefore, we focused on targeted drugs exhibiting higher efficacy in the patient samples. We observed significantly higher efficacy of both multi tyrosine kinase inhibitors masitinib and dasatinib (Fig S1b) in patient samples compared to the cell lines. These two drugs inhibit *KIT* among other target genes, and hence belong to the same drug class, thus increasing the confidence of the finding.

We next explored drug sensitivities of targeted drugs in relation to common driver mutations in AML. Some of the common AML-related mutations e.g., *KRAS*, *NRAS*, *EZH2*, *TP53* were more common in cell lines whereas *FLT3-ITD*, *DNMT3A*, *NPM1*, *IDH1*, *IDH2* mutations were more common in the patient samples (Fig S2). Unsupervised hierarchical clustering of 114 targeted sensitive drugs demonstrated mutation-based subgroups among the patient samples (Fig S3a) and the cell lines (Fig

S3b). Dasatinib was found to be in the same cluster as other tyrosine kinase inhibitors e.g. axitinib, imatinib, masitinib in patient samples. However, the dasatinib response was distinct from the other tyrosine kinase inhibitors in AML cell lines.

Next, the percentage of responders was calculated for individual drugs in both cell lines and patient samples to estimate drug efficacy in individual samples. A drug was defined as effective if its dDSS value exceeded the 95% quantile (8.5) of the overall dDSS distribution (Fig S4a). We then compared the percentage of responders ($\text{dDSS} \geq 8.5$) in both patient samples and cell lines across 224 targeted drugs (Fig 1b). The analysis revealed that dasatinib was one of the drugs that exhibited remarkable differential sensitivity in AML patient samples compared to the cell lines. We found 20% (9 out of 45) AML patient samples and 11% (3 out of 28) of cell lines were sensitive to dasatinib. Next, we assessed whether the dasatinib sensitivity was dependent on cell viability during assay but found no remarkable association using the patient samples (Figure S4b). Thus, dasatinib exhibited consistently higher efficacy in the patient samples as compared to the cell lines.

Next, we sought to identify molecular biomarkers for dasatinib sensitivity. We found no significant association between the *ex vivo* efficacy of dasatinib and the presence of any of the common driver mutations in the AML patient samples (Figure S5a). None of the AML patient samples had a mutation in the dasatinib target gene *KIT* (Fig S3a). Neither did we see any associations of *ex vivo* dasatinib response with clinical features of the disease (Figure S5b). We analyzed gene expression levels of dasatinib target proteins and found no significant correlation with dasatinib response either in the patient samples (Fig S5c) or in cell lines (Fig S5d). We then analyzed gene expression

levels in terms of deregulated pathways using gene set variation analysis (GSVA)¹⁴ and applied FDR to define KIT enrichment scores and their confidence levels (Fig 2a, Table S8). The KIT pathway gene signature derived from the REACTOME pathway database included 16 genes; *FYN*, *KITLG*, *CBL*, *SH2B3*, *PTPN6*, *SOS1*, *PRKCA*, *KIT*, *SH2B2*, *SOCS6*, *YES1*, *GRB2*, *LCK*, *SOCS1*, *SRC*, *LYN*. The majority of the genes encode for tyrosine kinases and signaling adaptor proteins (Table S9). Comparison of dasatinib sensitive and non-sensitive AML patients showed that the KIT pathway upregulation was a strong predictor for *ex vivo* dasatinib efficacy in AML (Fig 2b), stronger than the expression of any of the dasatinib targets alone. While KIT pathway upregulation is a stronger molecular determinant of *ex vivo* dasatinib efficacy than mutations or clinical features, its potential utility to assign dasatinib treatment for AML needs additional information.

Given the strong relationship between dasatinib sensitivity and KIT pathway upregulation, we then assessed if this effect is mediated through *KIT* as one of the targets. *KIT* gene is one of the sixteen genes of the KIT pathway. KIT (CD117) is a receptor tyrosine kinase expressed on the cell surface. We investigated the effect of dasatinib treatment on KIT protein expression and the induction of apoptosis to further define the effects of dasatinib in AML cell lines. The KIT targeting drugs dasatinib, masitinib, axitinib and imatinib (Fig S6a) was strongly effective in GDM-1, where the KIT pathway was also strongly and significantly upregulated (Fig S6b). We found reduced surface levels of KIT in dasatinib-treated GDM-1 cells as well as in *KIT*-mutant KASUMI-1 cells (positive control). In contrast, no such effect was seen after dasatinib treatment in MOLM-16 cells that are dasatinib-resistant and have no KIT pathway upregulation (Fig 2c). We also observed increased intracellular levels of

cleaved caspase 3 in KASUMI-1 and GDM-1 upon dasatinib treatment, compared to the responses in MOLM-16 cells (Fig 2d), indicating that dasatinib treatment-induced apoptosis (Fig S6c). Our findings are consistent with an earlier report suggesting dasatinib treatment reduces cell surface expression of KIT due to endocytosis in AML cells¹⁵. These results, therefore, suggest that the effects of dasatinib on AML cell viability and apoptosis could be mediated via the downregulation of the KIT protein. However, the overall gene expression profiles linked to the entire KIT pathway provided the strongest value as a drug response biomarker for predicting dasatinib response.

We also assessed KIT pathway enrichment scores in three chemo-refractory AML patients (AML_11, AML_36 and AML_41) treated with dasatinib to further explore the clinical relevance of the finding. Dasatinib was selected for clinical translation as a drug of choice for these patients based on leukemia-selective dasatinib response in *ex vivo* DSRT (Fig S7a) at Helsinki University Hospital². In two patients characterized by *ex vivo* dasatinib sensitivity and significant KIT pathway upregulation, dasatinib treatment led to complete remission (AML_36) and complete remission with incomplete hematological recovery (AML_41). In patient case AML_11, which also showed *ex vivo* dasatinib sensitivity but no upregulation of KIT pathway, no response to dasatinib was observed during a short treatment period which was limited by toxic side effects. (Fig 2e, S7b, c). Therefore, the patient data is also suggestive that KIT pathway activity could define AML patients who are most likely to respond to and benefit from dasatinib treatment.

171 Taken together, the combination of *in vitro*, *ex vivo* and clinical data suggest that gene
172 expression-based KIT pathway upregulation could act as a biomarker of dasatinib
173 efficacy in AML. We suggest that the upregulation of the KIT pathway in combination
174 with *ex vivo* dasatinib sensitivity testing could help to define patients who are most
175 likely to benefit from this treatment, a hypothesis to be tested in the form of a clinical
176 study.

Acknowledgements

We are grateful to the patients who donated samples to the study and thank the FIMM High Throughput Biomedicine Unit and Breeze DSRT data analysis pipeline teams for their support. The research was funded by the Finnish Cultural Foundation (DM), the Blood Disease Foundation Finland (DM), Finnish Hematology Association SHY (DM, AK), Ida Montinin Foundation (DM), EMBO short-term fellowship (AK), the Academy of Finland (Center of Excellence for Translational Cancer Biology; grants 310507, 313267, 326238 to TA; 277293 to KW; iCAN Digital Precision Cancer Medicine Flagship grant 1320185 to TA, CH), Cancer Society of Finland (DM, AK, OK, TA, KW, CH), Sigrid Jusélius Foundation (to OK, KP, TA and KW), EU Systems Microscopy (FP7) and TEKES/Business Finland (to OK and KP), Novo Nordisk Foundation (to KW; NNF17CC0027852). OK supported by Knut and Alice Wallenberg Foundation, Swedish Foundation for Strategic Research, VR environment grant. MK supported by University of Helsinki and Finnish Medical Foundation.

Authorship contribution

DM, AM and OK designed the study. DM and AM performed drug testing experiments. DM, BY and AK analyzed and visualized the data. DM generated hypotheses and interpreted results. DM and KJ designed and performed flow cytometry experiments. MK performed cell line variant calling and SP performed drug response data quality analysis. DM wrote the manuscript. MKo and KP obtained ethical permits, collected clinical samples and administered therapies. KP, MKo, TA, MW, KW, CH, AM and OK provided critical review. All authors contributed to and approved the final version of the manuscript.

Figure legends

Figure 1. Dasatinib has high sensitivity in AML patient samples compared to AML cell lines. **A)** Comparison of 290 drug responses between 45 AML patient samples and 28 AML cell lines. The median values of drugs plotted on the x-axis and negative log₁₀ of p-values plotted on the y-axis, where the statistical significance was calculated using the Wilcoxon rank-sum test. Dot colors indicate significant drugs (FDR <0.1) with high sensitivity in patient samples (orange) and cell lines (blue). **B)** Correlation of percent responders for 224 targeted drugs between 28 AML cell lines (x-axis) and 45 AML patient samples (y-axis). The highlighted drugs depict outliers based on percent responders above 15 percentage for AML patient samples and below 15 percentage for AML cell lines (the red dotted lines).

Figure 2. KIT pathway enrichment is associated with dasatinib efficacy. **A)** KIT pathway enrichment scores aligned to dasatinib response (dDSS). The dotted line represents sensitivity cut-off at 8.5 based on overall dDSS distribution. The asterisk marks represent significance levels as false discovery rates (FDR). **B)** KIT pathway enrichment scores in dasatinib sensitive (dDSS>8.5) and non-sensitive (dDSS<8.5) patient samples. **C)** Flow cytometry analysis represents the percentage of KIT positive cells in untreated (DMSO control) and 500nM dasatinib treated KASUMI-1, GDM-1 and MOLM-16 cells. **D)** Flow cytometry analysis represents the percentage of cleaved caspase 3 positive cells in untreated (DMSO control) and 500nM dasatinib treated KASUMI-1, GDM-1 and MOLM-16 cells. **E)** *Ex vivo* dasatinib response and matched KIT pathway in three AML patient cases who were given dasatinib treatment. The clinical outcomes of the treatment defined as a resistant disease (RD), complete

225 remission (CR) and complete remission with incomplete hematological recovery (CRi)
226 for all patients.

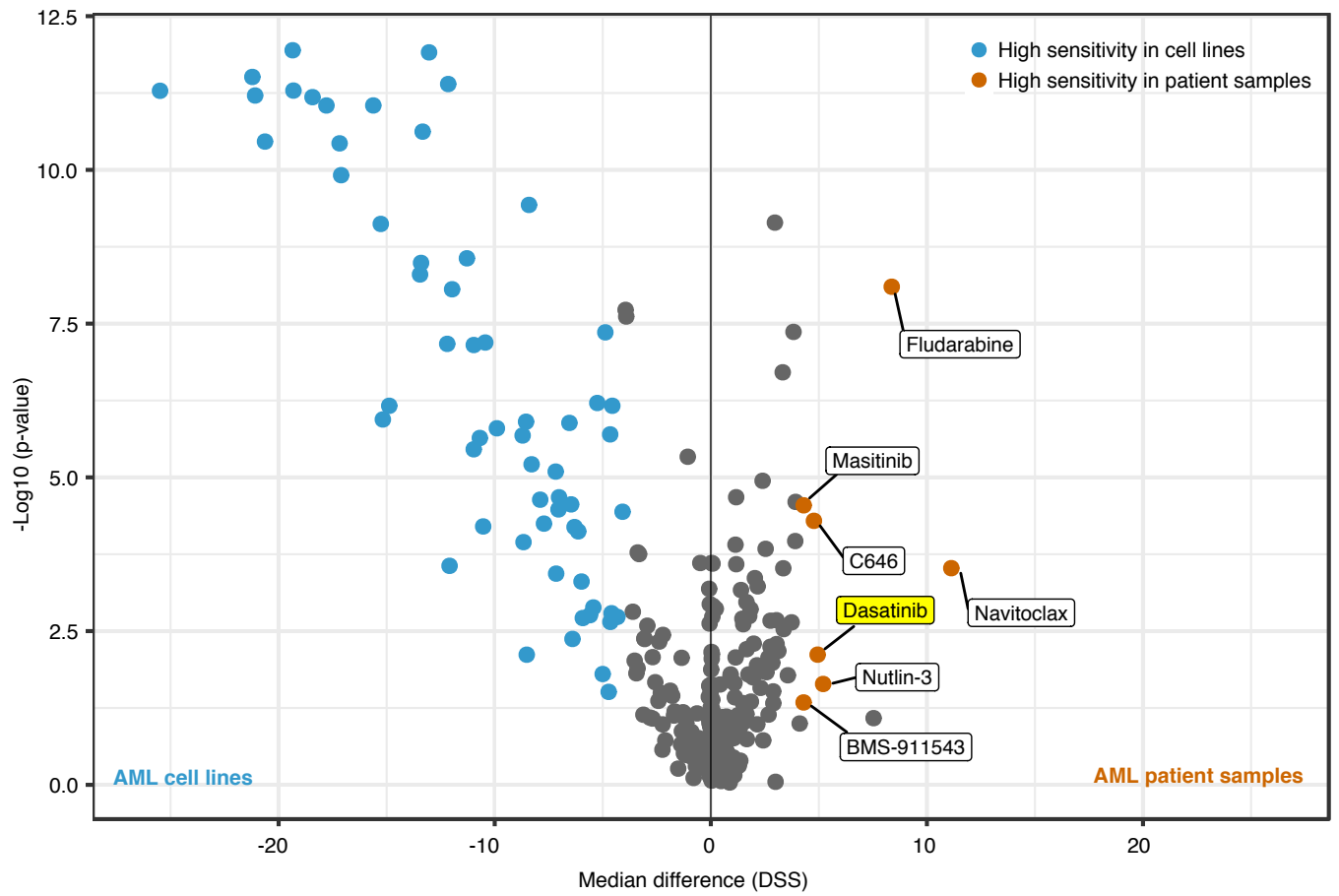
References

1. Döhner H, Estey E, Grimwade D, Amadori S, Appelbaum FR, Büchner T, *et al.* Diagnosis and management of AML in adults: 2017 ELN recommendations from an international expert panel. *Blood* 2017; **129**(4): 424-447.
2. Pemovska T, Kontro M, Yadav B, Edgren H, Eldfors S, Szwajda A, *et al.* Individualized Systems Medicine Strategy to Tailor Treatments for Patients with Chemorefractory Acute Myeloid Leukemia. *Cancer Discovery* 2013; **3**(12): 1416-1429.
3. Tyner JW, Tognon CE, Bottomly D, Wilmot B, Kurtz SE, Savage SL, *et al.* Functional genomic landscape of acute myeloid leukaemia. *Nature* 2018 2018/10/17.
4. Snijder B, Vladimer GI, Krall N, Miura K, Schmolke A-S, Kornauth C, *et al.* Image-based ex-vivo drug screening for patients with aggressive haematological malignancies: interim results from a single-arm, open-label, pilot study. *The Lancet Haematology* 2017; **4**(12): e595-e606.
5. Malani D, Murumagi A, Yadav B, Kontro M, Eldfors S, Kumar A, *et al.* Enhanced sensitivity to glucocorticoids in cytarabine-resistant AML. *Leukemia* 2017 May; **31**(5): 1187-1195.
6. Wilding JL, Bodmer WF. Cancer cell lines for drug discovery and development. *Cancer Research* 2014; **74**(9): 2377-2384.
7. Garnett MJ, Edelman EJ, Heidorn SJ, Greenman CD, Dastur A, Lau KW, *et al.* Systematic identification of genomic markers of drug sensitivity in cancer cells. *Nature* 2012; **483**(7391): 570-575.
8. Barretina J, Caponigro G, Stransky N, Venkatesan K, Margolin AA, Kim S, *et al.* The Cancer Cell Line Encyclopedia enables predictive modelling of anticancer drug sensitivity. *Nature* 2012; **483**(7391): 603-607.
9. Ghandi M, Huang FW, Jané-Valbuena J, Kryukov GV, Lo CC, McDonald ER, *et al.* Next-generation characterization of the Cancer Cell Line Encyclopedia. *Nature* 2019; **569**(7757): 503-508.
10. Lee S-I, Celik S, Logsdon BA, Lundberg SM, Martins TJ, Oehler VG, *et al.* A machine learning approach to integrate big data for precision medicine in acute myeloid leukemia. *Nature Communications* 2018; **9**(1): 42.
11. Iorio F, Knijnenburg TA, Vis DJ, Bignell GR, Menden MP, Schubert M, *et al.* A Landscape of Pharmacogenomic Interactions in Cancer. *Cell* 2016 Jul 28; **166**(3): 740-754.
12. Yadav B, Pemovska T, Szwajda A, Kuleskiy E, Kontro M, Karjalainen R, *et al.* Quantitative scoring of differential drug sensitivity for individually optimized anticancer therapies. *Scientific reports* 2014; **4**: 5193.

- 277 13. Kumar A, Kankainen M, Parsons A, Kallioniemi O, Mattila P, Heckman CA.
278 The impact of RNA sequence library construction protocols on transcriptomic
279 profiling of leukemia. *BMC genomics* 2017; **18**(1): 629-629.
280
- 281 14. Hänzelmann S, Castelo R, Guinney J. GSVA: gene set variation analysis for
282 microarray and RNA-Seq data. *BMC Bioinformatics* 2013; **14**(1): 7.
283
- 284 15. Heo S-K, Noh E-K, Kim JY, Jeong YK, Jo J-C, Choi Y, *et al.* Targeting c-KIT
285 (CD117) by dasatinib and radotinib promotes acute myeloid leukemia cell
286 death. *Scientific Reports* 2017; **7**(1): 15278.

Figure 1

A



B

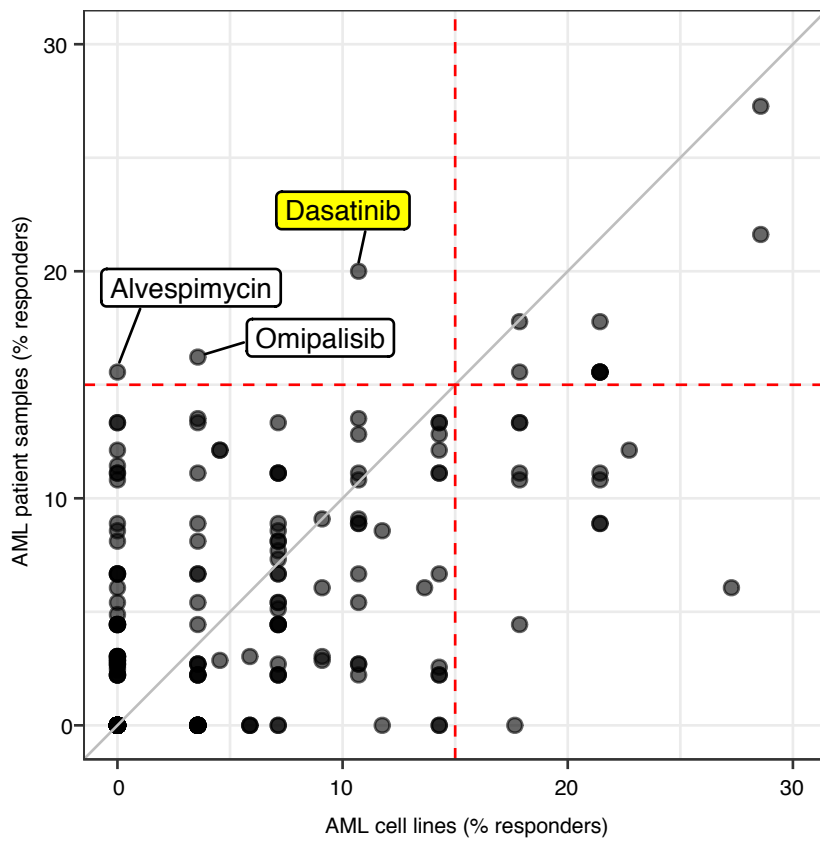
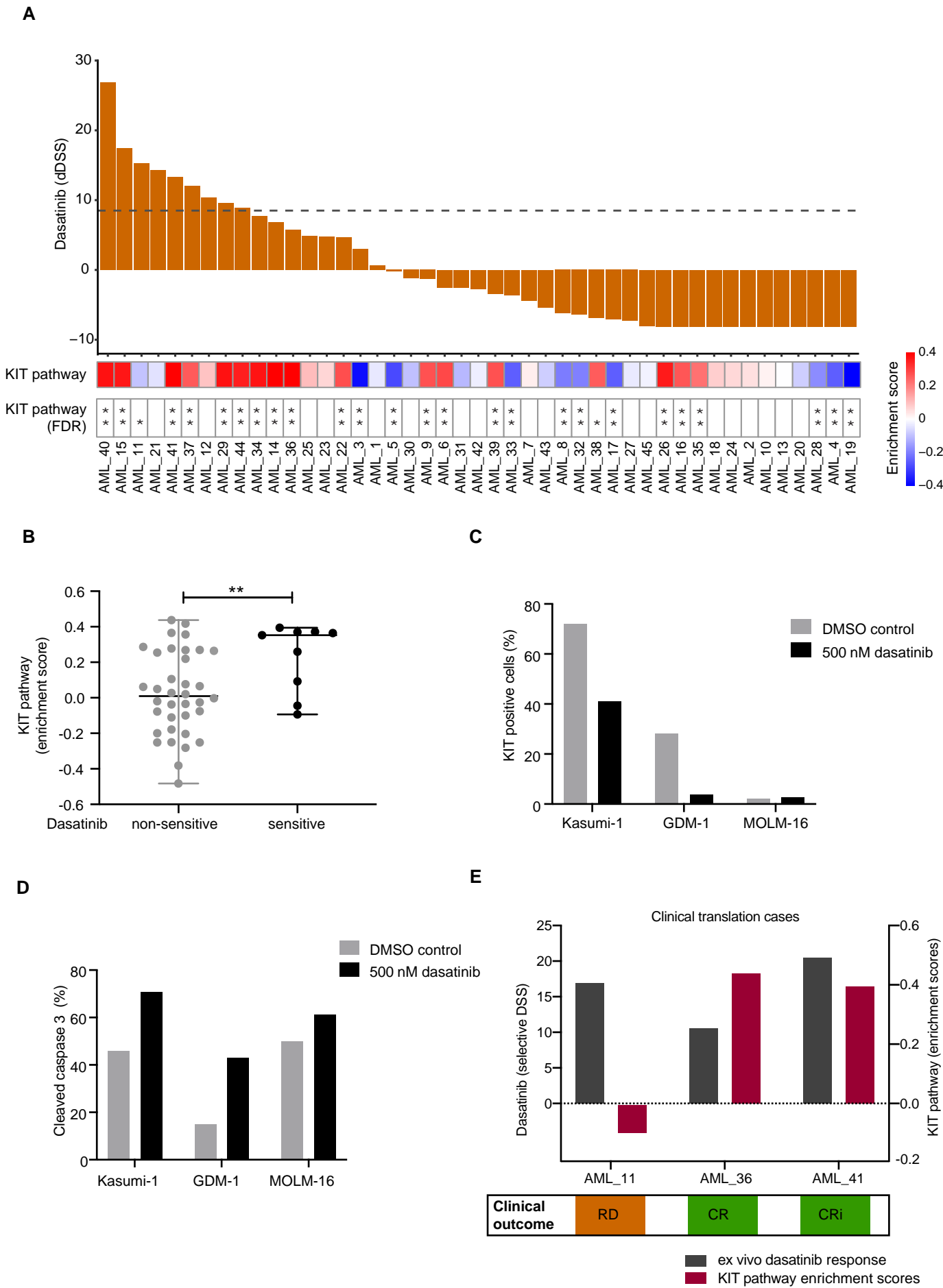


Figure 2



1 **KIT pathway upregulation predicts dasatinib efficacy in acute myeloid leukemia**

2

3 Disha Malani¹, Bhagwan Yadav¹, Ashwini Kumar¹, Swapnil Potdar¹, Mika Kontro^{1,2,3}, Matti
4 Kankainen², Komal K. Javarappa¹, Kimmo Porkka^{2,3}, Maija Wolf¹, Tero Aittokallio^{1,4}, Krister
5 Wennerberg^{1,5}, Caroline A. Heckman¹, Astrid Murumägi¹, Olli Kallioniemi^{1,6}

6

7 1. Institute for Molecular Medicine Finland (FIMM), HiLIFE, University of Helsinki, Helsinki,
8 Finland

9 2. Hematology Research Unit Helsinki, University of Helsinki, Helsinki, Finland

10 3. Department of Hematology, University Hospital Comprehensive Cancer Center, Helsinki, Finland

11 4. Department of Cancer Genetics, Institute for Cancer Research, Oslo University Hospital, and Oslo
12 Centre for Biostatistics and Epidemiology, University of Oslo, Oslo, Norway

13 5. Biotech Research & Innovation Centre, BRIC and Novo Nordisk Foundation Center for Stem Cell
14 Biology, DanStem, University of Copenhagen, Copenhagen, Denmark

15 6. Science for Life Laboratory, Department of Oncology and Pathology, Karolinska Institutet, Solna,
16 Sweden

17 **Supplementary figure legends:**

18 **Figure S1. A)** Percentage increment at 72h compared to 0h in terms of luminescence-based cell
19 viability during drug testing experiment for *ex vivo* AML patient samples and AML cell lines. **B)**
20 Comparison of drug sensitivity scores (DSS) for dasatinib between 45 AML patient samples and 28
21 AML cell lines. The Wilcoxon rank-sum test was applied to calculate p-value.

22
23 **Figure S2.** Mutation frequencies of 23 AML related driver genes in 45 patient samples and in 28
24 AML cell lines where FLT3-ITD represents internal tandem duplication and FLT3-PM represents
25 point mutations in FLT3 gene.

26
27 **Figure S3.** Unsupervised hierarchical clustering responses of 114 targeted sensitive drugs and **A)** 45
28 AML patient samples or **B)** 28 AML cell lines. The key AML related mutations annotated for both
29 patient samples and cell lines.

30
31 **Figure S4. A)** Distribution of differential drug sensitivity scores (dDSS) of 290 drug responses from
32 45 AML patient samples and 28 AML cell lines. Significant dDSS cut off 8.5 was defined as a 95%
33 quantile of the overall distribution. **B)** Upper panel depicts response to dasatinib (dDSS and lower
34 panel illustrates cell viability measured during drug testing assay in absence of drug (72 hours) for
35 37 AML patient samples.

36
37 **Figure S5. A)** Comparison of dasatinib response (DSS) between wild type and mutated samples for
38 *FLT3*-PM (point mutation), *FLT3*-ITD (internal tandem duplication), *NPM1*, *NRAS*, *PTPN11*,
39 *DNMT3A* using nonparametric Mann-Whitney test, where ns represents non-significant p-values. **B)**
40 Pearson correlation of age with dasatinib response. Comparison of the clinical features with dasatinib
41 responses using Mann-Whitney test, where ns represents non-significant p-values. **C)** Expression of

42 dasatinib target genes aligned to dasatinib response in 45 AML patient samples. The bar plot on the
43 right side depicts the Pearson correlation values between dasatinib response (dDSS) and RNA-seq
44 derived expression values (log₂ count per million (CPM)) of individual genes **D)** Expression (log₂
45 CPM) of dasatinib target genes aligned to dasatinib response (dDSS) in 21 AML cell lines.
46

47 **Figure S6. A)** dDSS for tyrosine kinase inhibitors (dasatinib, masitinib, axitinib and imatinib) in
48 AML cell lines GDM-1, KASUMI-1 and MOLM-16. **B)** Enrichment score for the KIT pathway
49 aligned to dasatinib response in 21 AML cell lines. The asterisk marks represent significance as false
50 discovery rates (FDR). **c.** The fluorescence signal of KIT antibody, cleaved caspase 3 antibody and
51 respective isotype control antibodies used for flow cytometry experiments.
52

53 **Figure S7. A)** Drug response profile of AML patient cases AML_11, AML_36 and AML_41
54 depicting the range of selective DSS (healthy bone marrow normalized DSS). Dasatinib is
55 highlighted in red. **B)** KIT pathway enrichment scores of AML patient samples where the patients
56 treated with dasatinib highlighted in red. **c.** Clinical information on drug treatment, disease status,
57 *ex vivo* dasatinib response and KIT pathway enrichment score for patients AML_11, AML_36 and
58 AML_41.

59 **Supplementary Text**

60

61 **AML patient samples and cell lines**

62 The samples were collected from AML patients (n=45) after signed informed consent using protocols
63 approved by local ethical committees (approvals 239/13/03/00/2010 and 303/13/03/01/2011).
64 Mononuclear cells were isolated from bone marrow aspirates and peripheral blood samples by Ficoll-
65 Paque (GE Healthcare) density gradient centrifugation. Twenty-eight AML cell lines were selected
66 across French American British (FAB) classes, ranging from M0 to M7 subtypes. The cell lines were
67 purchased from German collection of microorganisms and cell cultures (DSMZ), except for HL-60
68 cell line that was purchased from American type tissue culture collection (ATCC) and HL-60_TB, a
69 subline of HL60, was purchased from NCI-Frederick cancer DCTD tumor/cell line repository.

70

71 **Chemical compound collection**

72 The collection of 290 chemical compounds including 144 FDA (U.S. Food and Drug Administration)
73 or EMA (European Medical Agency) approved drugs, 112 investigational compounds and 34
74 chemical probes. The collection consists of conventional chemotherapy drugs, kinase inhibitors,
75 apoptosis modifiers, epigenetic modifiers, differentiating agents, metabolic modifiers, hormonal
76 therapeutics, and immunomodulators. The annotation for mechanism of actions or molecular targets
77 are given for each drug. The drugs were defined as sensitive if the dDSS was >8.5 for at least one cell
78 line or patient sample.

79

80 **Drug Sensitivity and Resistance Testing (DSRT)**

81 All cell lines were cultured in vendor specified media, except for HL-60 and HL-60_TB, which were
82 cultured in 90% RPMI 1640 with 10% FBS and Penicillin/Streptomycin. DSRT was performed with
83 the cell lines and freshly isolated mononuclear cells from bone marrow or blood of 45 diagnostic and

relapsed AML patients in mononuclear cell medium (Promocell) using the protocol described earlier¹. Briefly, the 290 compounds were dissolved in DMSO and dispensed in 384 well cell culture plates using an Echo 550 acoustic liquid handling system (Labcyte). Each compound was plated at five increasing concentrations, covering 10 000-fold range, mostly from 1-10 000nM. The drug plates were stored in nitrogen gas pressurized pods (Roylan Development Ltd.) before use. Cell seeding density was optimized prior to DSRT experiments for each cell line whereas patient samples were plated at 10000 cells per well. Cells were plated in pre-drugged plates and incubated for 72h at 37°C in 5% CO₂. Cell viability was measured using CellTiter Glo (Promega) reagent with PHERAstar FS (BMG Labtech) plate reader. Negative control DMSO and positive control benzethonium chloride were included in each assay plate for normalization of cell viability readouts (inhibition %).

Drug response data analysis

The drug response data was analyzed using FIMM in-house Breeze pipeline². Individual dose response curves and IC₅₀ values were calculated for each drug using the FIMM DSRT data analysis pipeline. Drug sensitivity scores (DSS), a modified area under dose-response curve, was calculated as described previously³. Differential drug sensitivity scores (dDSS) were calculated for each drug separately by subtracting the mean DSS over all the samples or over all the cell lines from the sample-specific DSS. The dDSS were calculated separately for cell lines and patient samples. Drug response data quality was assessed with Z-prime score, where variation was calculated between multiple positive and negative controls from the same plate.

Wilcoxon rank-sum test was performed with DSS to identify the drugs with significant differential efficacy between AML patient samples compared to the cell lines. The false discovery rates (FDR) were calculated using Benjamini & Hochberg method⁴. Median DSS difference <-4 or >4 and FDR <0.1 were considered significant for differential efficacy of drugs. The sensitivity was defined if

dDSS was above 8.5, which corresponds to the 95% quantile of the overall dDSS distribution over all the cell lines and patient samples. The percentage responders were calculated for a given drug with percent sensitive cell lines or patient samples. Targeted sensitive drugs (n=114) were defined if dDSS value were above 8.5 in at least one of the samples, which corresponds to the 95% quantile of the overall dDSS distribution over all the cell lines and patient samples. Unsupervised hierarchical clustering with complete linkage was performed using Euclidean distance for cell lines and patient samples, and correlation distance for dDSS profiles of compounds.

DNA sequencing and somatic variant analysis

Exome sequencing was performed using DNA isolated from mononuclear cells of AML patient samples (n=45) and matching skin biopsies from the same patients using Agilent or Roche NimbleGen exome capture kits and a HiSeq 2500 instrument (Illumina). The data processing and variant calling was performed using same pipeline as described previously¹. Genomic DNA was isolated from the cell lines (n=28) using the DNeasy Blood and Tissue Kit (Qiagen). Massive parallel-targeted sequencing of 578 genes was performed using Nimblegen's SeqCap EZ Designs kit (Roche). 2 µg of DNA was used for library preparation, enrichment and sequencing using HiSeq 2500 (Illumina).

Genetic variants in each cell line were called and annotated as described earlier⁵. Briefly, variants were called using a modified GATK best-practice and annotated using Annovar tool against RefGene database. Subsequently, the variants called from the cell lines were filtered by removing variants not passing variant calling filters, not located in exonic or splice region synonymous SNVs and frameshift insertion and deletions. Furthermore, variants were removed if not found in hematopoietic malignancies in the COSMIC version 87 (<https://cosmic-blog.sanger.ac.uk/cosmic-release-v87>), or not annotated in the BeatAML dataset, which includes variants detected in 600 AML patient

134 samples⁶. Finally, variants were removed if the variant's frequency was > 1% in gnomAD database
135 of healthy individuals when considering all populations (<https://gnomad.broadinstitute.org>), if
136 supported by <10 reads in total and <2 reads in either direction, having a variant allele frequency
137 <2%, and having a strand odd ratio for SNVs ≥ 3.00 , and strand odd ratio for indels ≥ 11.00 and
138 quality <40.

139

140 **RNA-sequencing**

141 RNA-sequencing was performed for 45 AML patient samples. Total RNA (2.5-5 μ g) was extracted
142 from bone marrow or peripheral blood mononuclear cells from AML patients using the miRNeasy or
143 AllPrep kit (Qiagen) and depleted of ribosomal-RNA (Ribo-ZeroTM rRNA Removal Kit, Epicentre)
144 after purification, reverse transcribed to double stranded cDNA (SuperScriptTM Double- Stranded
145 cDNA Synthesis Kit, Thermo Fisher). Library quality was evaluated on high sensitivity chips using
146 the Agilent Bioanalyzer (Agilent Technologies). Paired-end sequencing with 100 bp read length was
147 performed using HiSeq 2500 (Illumina) as described previously⁷.

148

149 **Gene expression analysis**

150 RNA-seq data pre-processing including, quality control, alignment, normalization, feature count and
151 count per million (CPM) calculation were performed as described previously⁷. Briefly, Trimmomatic⁸
152 was used to correct reads for low quality, Illumina adapters, and short read-length. Filtered paired-
153 end reads were aligned to the human genome (GRCh38) using STAR aligner⁹ with the guidance of
154 EnsEMBL v82 gene models. Feature counts were computed using SubRead¹⁰ R-package and
155 converted to expression estimates using Trimmed Mean of M-values (TMM) normalization method
156 ¹¹. Default parameters were used with exception that reads were allowed to be assigned to overlapping
157 genome features in the feature counting. The published RNA-seq data (raw read counts) for 21 AML

cell lines was obtained from the CCLE resource¹². Raw reads were further normalized by TMM method and log₂ CPM values were calculated similar to the patient samples.

Pathway enrichment analysis

To get the pathway enrichment scores, the gene expression values (log₂ CPM) for the protein coding genes were subjected to the gene set variation analysis (GSVA) using a R-package (GSVA version 1.18.0)¹³ for both 45 AML patient samples and 21 cell lines. The GSVA analysis calculates the relative enrichment of a gene set across the sample set. We applied GSVA analysis separately for patient samples and cell lines. The pathway gene set signatures were obtained from the Molecular Signatures Database (MSigDB) (<https://www.gsea-msigdb.org/gsea/msigdb/collections.jsp#C1>) database version “c2.cp.reactome.v6.2.entrez.gmt”. The canonical pathways were derived from REACTOME database (n=674 gene sets), where we specifically focused on “REACTOME_REGULATION_OF_KIT_SIGNALING” based on prior knowledge. A high enrichment score represents upregulated pathway, whereas low or negative scores represent downregulated pathways. We applied 1000 bootstrap iterations on GSVA scores in order to get the significance levels. Next, the p-values were adjusted across the patient sample or across the cell lines by applying Benjamini and Hochberg (BH) method to get false discovery rates (FDR). The FDR < 0.05 was considered significant. The KIT pathway gene signature consists of 16 genes; *FYN*, *KITLG*, *CBL*, *SH2B3*, *PTPN6*, *SOS1*, *PRKCA*, *KIT*, *SH2B2*, *SOCS6*, *YES1*, *GRB2*, *LCK*, *SOCS1*, *SRC*, *LYN*. The KIT pathway enrichment scores ranged from -0.482 to 0.437 in case of AML patient samples (n=45) and from -0.431 to 0.525 in AML cell lines (n=21).

Flow cytometry analysis

Dasatinib and venetoclax were purchased from LC Laboratories and ChemieTek, respectively, and dissolved in DMSO to prepare 10 mM stocks. The KASUMI-1, GDM-1 and MOLM-16 cells were

183 treated with 100 nM and 500 nM dasatinib and 100 nM venetoclax (a positive control for apoptosis
184 induction) for 24 h in V-bottom 96 well plates (Nunc). After the incubation, the plate was centrifuged
185 at 600 g for 4 min and supernatant was discarded. The cells were stained with 1:1000 dilution of
186 zombie violet (BioLegend) as per the vendor's instructions. The cells were washed with 1X PBS and
187 stained with 1:50 dilution of CD117(cKIT)-BV605 antibody (562687, BD Biosciences). The cells
188 were washed with 1X PBS and fixed using 2.5% formaldehyde for 10 min at 37°C and permeabilized
189 using 70% cold methanol for 20 min at 4°C. Subsequently the washed cells were stained with 1:50
190 dilution of cleaved caspase 3-A647 antibody (9602, Cell Signaling Technology). The isotype control
191 antibodies BV605 (562652, BD Biosciences) and A647(612599, BD Biosciences) were used at same
192 concentration as the CD117 and cleaved caspase 3 antibodies. CD117 antibody stained UltraComp
193 beads (01-2222-41, Invitrogen) and cleaved caspase 3 stained venetoclax treated Kasumi-1 cells were
194 used for compensation. An iQue Plus (Intellicyte) flow cytometer was used to measure florescence
195 of the stained cells and beads. The compensated data were analyzed using FlowJo™ software
196 (<https://www.flowjo.com/>).

197

198 **Clinical Translation in AML patients**

199 We have established leukemia precision medicine program to tailor targeted therapies based on top
200 selective drug responses using functional testing and molecular profiles¹. The program is a
201 collaborative effort involving biologists, bioinformaticians and clinicians at Institute for Molecular
202 Medicine Finland (FIMM) and Helsinki University Hospital. The program is primarily for end-stage
203 chemo-refractory AML patients and in exceptional conditions for diagnostic primary AML patient
204 cases. The treatment regimens comprised of approved non-AML drugs were used as a single agent
205 or in combinations for clinical translation in individual AML patient cases, including serial therapy
206 with different regimens in some of the patients. The drugs classified as signaling molecule inhibitors,
207 immunomodulator, proteasome inhibitor and epigenetic modifier, were approved for cancer

208 indications and patients were treated under off label compassionate usage. The regimens resulted in
209 either complete remission (CR), complete remission with incomplete hematological recovery (CRi)
210 or resistant disease (RD) defined by ELN2017 criteria¹⁴. Patient AML_11 was given dasatinib in
211 combination with azacytidine and was resistant to the therapy. Patient AML_36 was given dasatinib-
212 azacitidine therapy and the patient was MDR positive after the therapy, however the blast count
213 decreased after the therapy was defined as CRi as per ELN2017 criteria. Patient_41 was given
214 combination of dasatinib (multi-tyrosine kinase inhibitor), temsirolimus (mTOR inhibitor) and
215 sunitinib (tyrosine kinase inhibitor) and achieved complete remission with the therapy. We assumed
216 that dasatinib response associated with KIT pathway, considering *ex vivo* association and *KIT* being
217 one of the target genes, gave biological meaningful hypothesis.

218

219 **Statistical Analyses**

220 The statistical analyses were performed and figures were generated using Prism software version 8
221 (GraphPad) and R version 3.3.3 (2017-03-06). Statistical dependence between two variables was
222 calculated using Pearson's correlation coefficient. The Wilcoxon rank-sum test was applied to assess
223 differences between drug responses.

224 References

- 225 1. Pemovska T, Kontro M, Yadav B, Edgren H, Eldfors S, Szwajda A, *et al.* Individualized
226 Systems Medicine Strategy to Tailor Treatments for Patients with Chemorefractory Acute
227 Myeloid Leukemia. *Cancer Discovery* 2013; **3**(12): 1416-1429.
228
- 229 2. Potdar S, Ianevski A, Mpindi JP, Bychkov D, Fiere C, Ianevski P, *et al.* Breeze: an
230 integrated quality control and data analysis application for high-throughput drug screening.
231 *Bioinformatics* 2020 Mar 2.
232
- 233 3. Yadav B, Pemovska T, Szwajda A, Kuleskiy E, Kontro M, Karjalainen R, *et al.*
234 Quantitative scoring of differential drug sensitivity for individually optimized anticancer
235 therapies. *Scientific reports* 2014; **4**: 5193.
236
- 237 4. Benjamini Y, Hochberg Y. Controlling the false discovery rate: a practical and powerful
238 approach to multiple testing. *Journal of the Royal statistical society: series B*
239 *(Methodological)* 1995; **57**(1): 289-300.
240
- 241 5. Dufva O, Kankainen M, Kelkka T, Sekiguchi N, Awad SA, Eldfors S, *et al.* Aggressive
242 natural killer-cell leukemia mutational landscape and drug profiling highlight JAK-STAT
243 signaling as therapeutic target. *Nature Communications* 2018 2018/04/19; **9**(1): 1567.
244
- 245 6. Tyner JW, Tognon CE, Bottomly D, Wilmot B, Kurtz SE, Savage SL, *et al.* Functional
246 genomic landscape of acute myeloid leukaemia. *Nature* 2018 2018/10/17.
247
- 248 7. Kumar A, Kankainen M, Parsons A, Kallioniemi O, Mattila P, Heckman CA. The impact of
249 RNA sequence library construction protocols on transcriptomic profiling of leukemia. *BMC*
250 *genomics* 2017; **18**(1): 629-629.
251
- 252 8. Bolger AM, Lohse M, Usadel B. Trimmomatic: a flexible trimmer for Illumina sequence
253 data. *Bioinformatics* 2014; **30**(15): 2114-2120.
254
- 255 9. Dobin A, Davis CA, Zaleski C, Schlesinger F, Drenkow J, Chaisson M, *et al.* STAR:
256 ultrafast universal RNA-seq aligner. *Bioinformatics* 2012; **29**(1): 15-21.
257
- 258 10. Liao Y, Smyth GK, Shi W. The Subread aligner: fast, accurate and scalable read mapping
259 by seed-and-vote. *Nucleic Acids Research* 2013; **41**(10): e108-e108.
260
- 261 11. Robinson MD, Oshlack A. A scaling normalization method for differential expression
262 analysis of RNA-seq data. *Genome Biol* 2010; **11**(3): R25.
263
- 264 12. Ghandi M, Huang FW, Jané-Valbuena J, Kryukov GV, Lo CC, McDonald ER, *et al.* Next-
265 generation characterization of the Cancer Cell Line Encyclopedia. *Nature* 2019; **569**(7757):
266 503-508.
267
- 268 13. Hänzelmann S, Castelo R, Guinney J. GSVA: gene set variation analysis for microarray and
269 RNA-Seq data. *BMC Bioinformatics* 2013; **14**(1): 7.
270

- 271 14. Döhner H, Estey E, Grimwade D, Amadori S, Appelbaum FR, Büchner T, *et al.* Diagnosis
272 and management of AML in adults: 2017 ELN recommendations from an international
273 expert panel. *Blood* 2017; **129**(4): 424-447.